Research Square

Preprints are preliminary reports that have not undergone peer review.
They should not be considered conclusive, used to inform clinical practice,
or referenced by the media as validated information.

An ingestible bioelectronic capsule for in vivo DNA monitoring in the gastrointestinal tract

Hanjie Wang

wanghanjie@hainanu.edu.cn

Hainan University

Guijie Bai

Tianjin University

Xin Huang

Tianjin University

Xinran Li

Hainan University

Yinli Bao

Longyan University

Hui Liu

Hainan University

Hongxiang Li

Tianjin University

Leilei Wang

Tianjin University

Xinyue Cao

Tianjin University

Maoxing Yang

Hainan University

Zhanpu Bin

Hainan University

Xufei Teng

Tianjin University

Meng Song

Hainan University

Jiachao Cao

Longyan University

Jiazhen Lu

Longyan University

Yi Zhang

Tianjin University
Yanning Zhang
Tianjin University
Long Li
Hainan University
Hanyan Zhou
Hainan University
Zhen Yang
Hainan University
Yue Jiang
Tianjin University
Chao Zhang
Tianjin University
Xi Jiang
Changhai Hospital
Dawei Sun
Tianjin University
Yihao Wang
Tianjin University
Haihan Yao
Tianjin University
Tiantian Hao
Tianjin University
Cuiqin Huang
Longyan University
Zhijie Feng
Hainan University
Duo Liu
Hainan University

Article

Keywords:

Posted Date: November 13th, 2026

DOI: https://doi.org/10.21203/rs.3.rs-10969336/v1

License: This work is licensed under a Creative Commons Attribution 4.0 International License.
Read Full License

Additional Declarations: There is **NO** Competing Interest.

An ingestible bioelectronic capsule for in vivo DNA monitoring in the gastrointestinal tract

Gujie Bai[1,2,#], Xin Huang[1,2,#], Xinran Li[1,2,#], Yinli Bao[4,#], Hui Liu[1,2,#], Hongxiang Li[1,2], Leilei Wang[2], Xinyue Cao[2], Maoxing Yang[1], Zhanpu Bin[1], Xufei Teng[2], Meng Song[1], Jiachao Cao[4], Jiazhen Lu[4], Yi Zhang[4], Yanning Zhang[2], Long Li[1,2], Hanyan Zhou[1,2], ZhenYang[1], Yue Jiang[1,2], Chao Zhang[1,2], Xi Jiang[5], Dawei Sun[1,2], YihaoWang[2], Haihan Yao[2], Tiantian Hao[2], Cuiqin Huang[4,*], Zhijie Feng[1,*], Duo Liu[1,3,*], Hanjie Wang[1,2,3,4,*]

[1] Key Laboratory of Tropical Biological Resources of Ministry of Education and Hainan Engineering Research Center for Drug Screening and Evaluation, School of Pharmaceutical Sciences, Hainan University, Haikou 570228, China.

[2] School of Life Sciences, Faculty of Medicine, Tianjin University, Tianjin 300072, China

[3] State Key Laboratory of Synthetic Biology, Tianjin University, Tianjin 300072, China.

[4] Engineering Research Center for the Prevention and Control of Animal Original Zoonosis of Fujian Province University, College of Life Science, Longyan University, Fujian 364012, China.

[5] Department of Gastroenterology, National Clinical Research Center for Digestive Diseases, Shanghai Key Laboratory of Nautical Medicine and Translation of Drugs and Medical Devices, Changhai Hospital; National Key Laboratory of Immunity and Inflammation, Naval Medical University, Shanghai, China.

[#]These authors contributed equally

[*]Corresponding author

Correspondence: cuiqinh@126.com (Cuiqin Huang), fengzhijie@hainanu.edu.cn (Zhijie Feng), liuduo@hainanu.edu.cn (Duo Liu), wanghanjie@hainanu.edu.cn (Hanjie Wang)

Abstract

Early detection of gastrointestinal pathogens and disease-associated DNA sequences is critical for timely clinical intervention, yet current diagnostic workflows rely on *ex vivo* stool analysis or invasive biopsy, which delays diagnosis and compromises trace DNA integrity. Here, we report an ingestible bioelectronic capsule embedded with a paper-based CRISPR/Cas system for *in vivo* sampling, on-board lysis, sequence-specific DNA sensing, and wireless signal readout. By performing thoroughly *in situ*, the capsule mitigates the degradation and dilution of target DNA that occur during *ex vivo* handling. It enables detection of the *Salmonella invA* gene in simulated gastric fluid, real gastric samples, and the stomachs of large animal models (canine and porcine). We further validate the capsule strategy for detecting *Helicobacter pylori* DNA in human volunteer samples. This CRISPR/Cas-embedded bioelectronic capsule offers a non-invasive, point-of-care approach for *in vivo* monitoring of specific DNA sequences in the gastrointestinal tract, with potential for personalized health management.

Introduction

Disease-related nucleic acid macromolecules in the gastrointestinal tract, such as pathogen DNA and tumor-associated aberrations, are highly specific and well-defined, making them valuable clinical diagnostic markers[1-3]. For example, *in vivo* sampling followed by *ex vivo* pathogen DNA detection guides antibiotic stewardship, whereas fecal testing for sequence aberrations enables early colorectal cancer risk stratification[4]. However, current reliance on *ex vivo* analysis after stool collection or invasive sampling inevitably delays diagnosis, risks losing trace DNA densities to degradation and dilution[5-7], and requires specialized facilities, altogether precluding routine, timely monitoring. The absence of an *in-vivo* monitoring strategy for gastrointestinal macromolecular DNA targets thus remains a critical bottleneck, especially for early warning of infections and malignancies, where rapid genetic insight is decisive.

Over the past decade, CRISPR-based gene-editing technologies have substantially improved nucleic acid recognition accuracy and programmability, enabling detection of diverse nucleic acid alterations[8-11]. Their integration with portable electronics has facilitated point-of-care testing, simplified procedures and reduced reliance on professional biomedical laboratories[12-15]. Yet ingestible CRISPR formats face even greater challenges than wearables in sample handling, biosensing, and automated processing, particularly given the complex gastrointestinal environment[16]. Meanwhile, recently developed electronic capsules offer viable platforms for wireless digital readout within the gut[17,18]. Current capsules can monitor physiological parameters (imaging, pH, slow waves) [19,20] and, via bacteria sensors or electrochemical biosensors, detect small biochemicals (heme[21], nitrogen oxides[22,23], glucose[24], ionic species, and serotonin[25]). Nevertheless, none of these systems are adapted for detecting macromolecular nucleic acids. Therefore, a capsule-like system

integrating CRISPR/Cas-based nucleic acid sensing with on-board signal processing would fill this void and make genuine genetic monitoring *in vivo* come true.

Based on the above considerations, we propose integrating nucleic acid sequence recognition into a miniaturized electronic device to construct a "CRISPR/Cas-embedded electronic capsule". The key hurdles include achieving *in vivo* mass transport of macromolecular DNA, performing specific recognition and digitized output signal readout, and ensuring overall system efficiency, fidelity, and stability. Current electronic capsules use size-exclusion membranes that allow only small biomolecules into the detection chamber, a strategy unsuitable for DNA and unable to handle intracellular targets[21,23,24]. Hence, the electronic capsule needs more open interfaces for active sampling and lysis processing. Moreover, establishing a CRISPR/Cas-based workflow inside the chamber, including DNA transport, enzyme-mediated biosensing, and readout acquisition, poses significant challenges. Stable coupling between CRISPR/Cas reactions and electronic components, especially the signal-transduction interface, is crucial for digitizing genetic information. Finally, integration of the entire system into a capsule platform shall perform with high efficiency and robustness in complex *in vivo* environments.

Motivated by these challenges, we construct an ingestible, closed-loop diagnostic bioelectronic capsule embedded with a paper-based CRISPR/Cas system. The platform establishes a continuous process from macromolecular DNA mass transport and specific recognition to reported signal readout, thereby converting characterized DNA information into readable digital signals. We choose the gastric environment as the primary testbed, as it is the first site encountered by pathogens entering via the digestive tract and also poses the

most severe threat to DNA integrity[6,26]. We construct a capsule specifically targeting the *Salmonella invA* gene and validate its performance both *in vitro* and *in vivo*. In order to approach real clinical application scenarios, we also develop the capsule strategy for detecting *Helicobacter pylori* DNA, holding important clinical value for early disease warning[27,28]. This CRISPR/Cas-embedded capsule platform provides a new avenue for *in-vivo* large biomolecular monitoring and gastrointestinal disease management.

Results

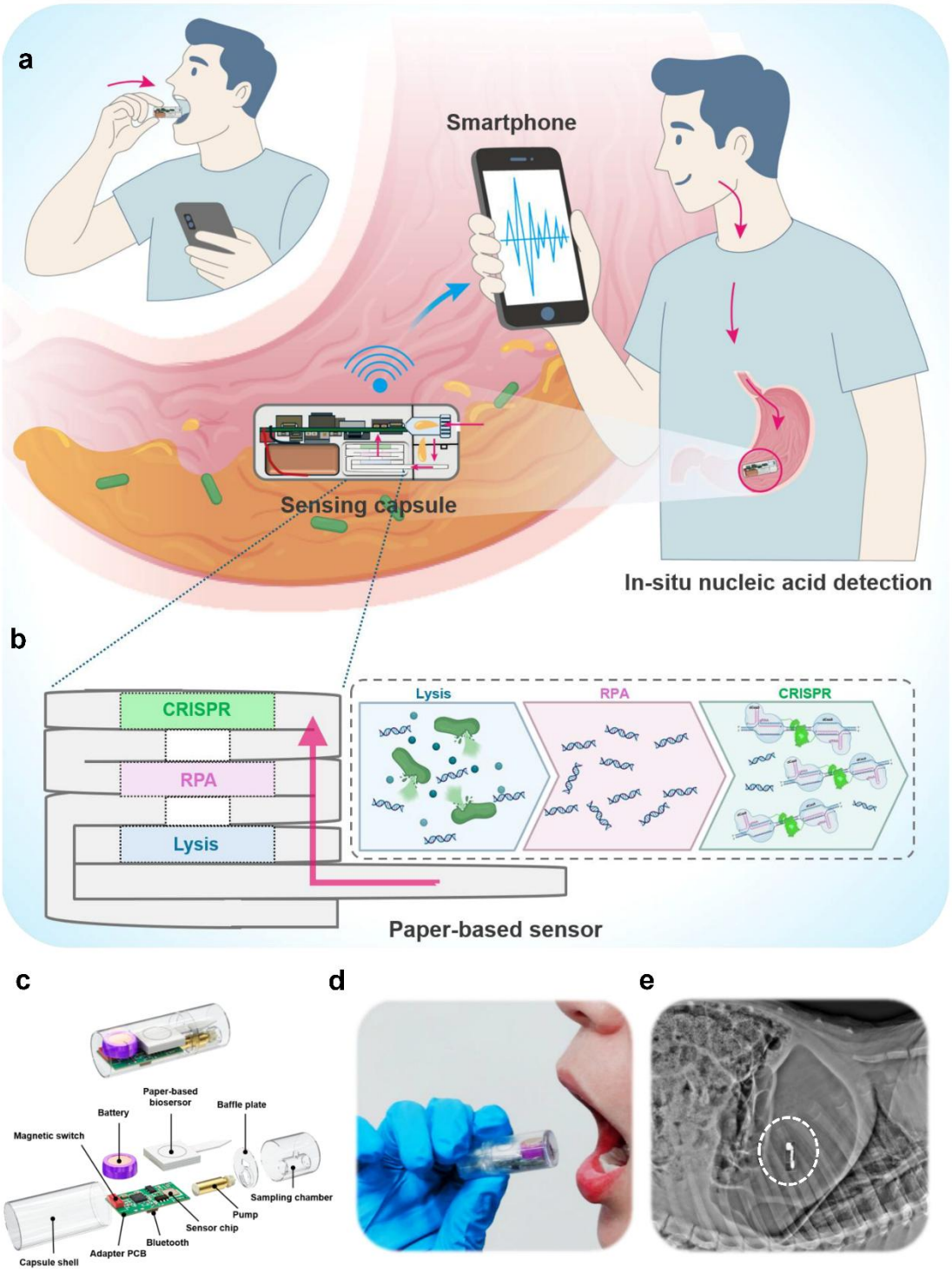
Design of the ingestible CRISPR/Cas-embedded bioelectronic capsule

Our vision is that, in daily scenarios, individuals can orally administrate a bioelectronic capsule to monitor characterized DNA (e.g. pathogen DNA) through *in vivo* sampling, detection, and digital readout. This capsule is expected to integrate a paper-based CRISPR/Cas module and electronic modules into a single platform, enabling the entire sample processing to be performed in the gastric environment and the monitoring results to be read timely on intelligent terminals (e.g. smartphone) (Figure 1a).

Upon entering the capsule, gastric samples will be absorbed on a paper-based substrate, where most fluid handling and biosensing occur (Figure 1b). In the lysis zone, pathogens are disrupted to release nucleic acids, which then migrate through a polyvinyl alcohol (PVA) delay into next recombinase polymerase amplification (RPA) zone for isothermal amplification of target sequences. A second PVA delay directs the products into the CRISPR/Cas zone, where dual catalytically dead Cas9 (dCas9)–single guide RNA (sgRNA) complexes recognize specific DNA targets. Target-induced assembly of split reporter domains restore NanoLuc luciferase activity, producing bioluminescence

proportional to target concentration. This light signal serves as the input for downstream photosensing, conversion, and wireless readout. The PVA structures ensure spatiotemporal automated sequential operations through the zones without external intervention and prevent cross-interference [29].

The configuration of capsule integrates several electronic modules, including a miniaturized pump, an integrated circuit equipped with Bluetooth, magnetic switch and battery (Figure 1c). This capsule constitutes a complete closed-loop process of oral delivery, *in vivo* gastric sampling and detection, and wireless readout, enabling an *in-vivo* diagnostic paradigm (Figure 1d, e). This platform is expected to overcome the limitations of conventional nucleic acid testing that depend on delayed fecal specimen detection, transportation, and bulky instrumentation.



146

147 **Figure 1. An ingestible electronic capsule for in situ gastric nucleic acid detection.**
148 **a**, Overview of the ingestible electronic capsule system for *in vivo* gastric nucleic acid
149 detection. Following oral ingestion and entry into the stomach, the capsule enables *in vivo*
150 nucleic acid detection within the gastric environment. **b**, Schematic illustration of the paper-
151 based nucleic acid sensor and its detection workflow. Grey regions indicate hydrophobic

barriers; blue, purple, yellow, green and white circles denote the lysis, recombinase polymerase amplification (RPA), chemiluminescent substrate, CRISPR detection and PVA delay regions, respectively. Pink arrows indicate the direction of liquid flow. **c**, Exploded view of the ingestible electronic capsule. **d**, Oral ingestion of the electronic capsule by a human volunteer. **e**, X-ray image showing the electronic capsule positioned in procine stomach. Panel b created with BioRender.com.

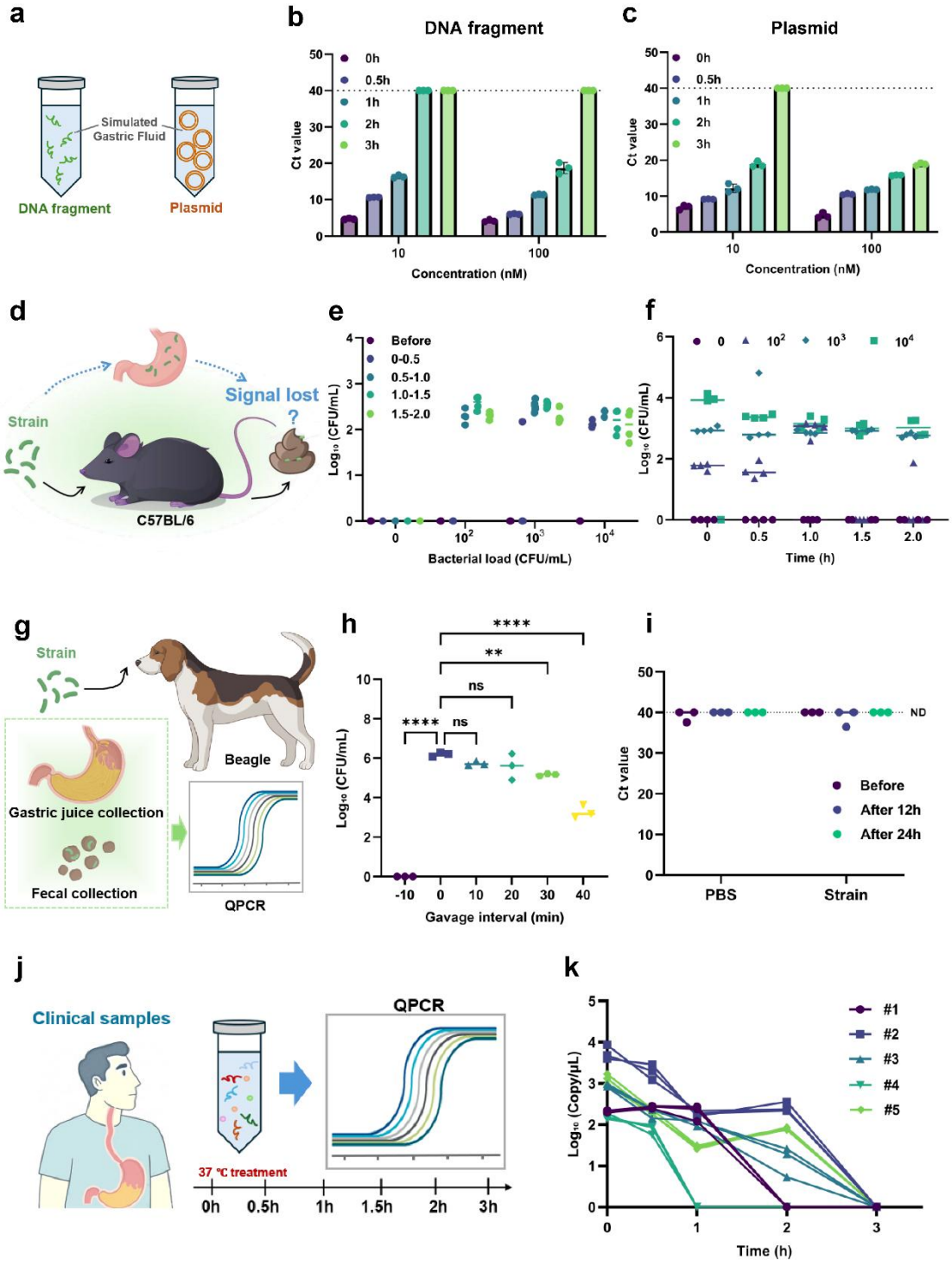
Evaluation of the necessity for in situ and timely DNA detection

A premise underlying our idea of *in-vivo* diagnostic capsule is that conventional fecal specimen detection may incur substantial loss of pathogenic DNA information density. To verify the above premise, we detected significant degradation of target pathogenic DNA in simulated gastric environment within hours[30,31] (Figures 2a-c). Then, we established a mouse model by oral gavage with varying densities of engineered *E. coli* strains integrated with *Salmonella invA* gene (Figure 2d). For the low densities of 1×10^2 and 1×10^3 CFU/mL, *invA* was undetectable or only partially detectable in the earliest batch of fecal samples following defecation, whereas higher density of 1×10^4 CFU/mL exhibited orders of magnitude of *invA* information loss (Figure 2e). We reasoned detecting pathogens timely during their gastrointestinal entry would be more reliable, and found that the *invA* information densities could be preserved in the gastric sampling specimens within 0.5 h. However, when sampling was extended, DNA information would also be severely lost (Figure 2f). The results were crossly validated by colony-counting data (Figure S1). These findings indicated that the timely *in vivo* gastric detection was essential for capturing pathogen DNA information.

To further verify the importance of *in vivo* gastric detection, we performed canine experiments (Figure 2g). To accommodate canine larger gastrointestinal

volume, a higher density of 1×10^6 CFU/mL strains was administered orally. Gastric fluid samples were endoscopically retrieved at 10-min intervals and immediately detected. As depicted in Figure 2h, Target DNA information density was restored within first 20 min but decreased by 1-3 orders of magnitude within 30-40 min. This reiterated that even with *in vivo* sampling coupled with *ex vivo* analysis, accurate quantification was restricted to a very narrow time window. By contrast, the faecal samples at 12 and 24 h post-gavage exhibited no detectable DNA information (Figure 2i). Further experiments were performed in a porcine model and gained similar results (Figures S2a-b). Collectively, these results reinforced the notion that reliance on downstream excretory specimens or delayed sample analysis introduced significant loss of DNA information.

Finally, to more closely approximate clinical reality, we evaluated the stability of *Helicobacter*-specific 16S rDNA in positive diagnostic samples of gastric fluid, which were collected using a biosafety sampling tube (Figure 2j). Following incubation at 37 °C for 2-3 h, target DNA signals were completely lost (Figure 2k). This indicated that delayed processing of positive *in vivo* specimens could significantly compromise critical DNA information. Together, these findings highlight the need for in situ sampling and measurement to preserve fragile biological information, providing a strong rationale for orally administered *in vivo* detection platforms.



201

202 **Figure 2. Temporal stability of pathogen-derived nucleic acids in gastric**
203 **environment. a**, Schematic illustration of the stability assessment of linear DNA fragments
204 and plasmids in simulated gastric fluid. **b-c**, Residual concentration detection of respective
205 10 nM and 100 nM linear DNA fragments of *Salmonella invA* gene (b) or plasmids
206 containing this gene (c) after incubation in simulated gastric fluid at 37 °C for different

durations. Dashed lines indicate undetected or above-threshold values. **d**, Schematic illustration of the assessment of pathogen-derived genetic information retention in mice following oral gavage. **e**, qPCR analysis of pathogen-derived signals retained in faecal samples from mice administered with different bacterial loads. **f**, qPCR quantification of pathogen loads in mouse gastric tissues collected at 0, 0.5, 1, 1.5 and 2 h after oral gavage. **g**, Schematic illustration of the assessment of pathogen retention in the stomach of dogs following oral gavage. **h**, qPCR quantification of pathogen loads in canine gastric fluid collected at 0, 10, 20, 30 and 40 min after oral gavage. **i**, qPCR quantification of pathogen-derived signals in faecal samples collected from dogs at 12 and 24 h after oral gavage. **j**, Schematic illustration of the assessment of DNA fragment stability in clinical gastric fluid samples. **k**, Quantification of DNA fragments in clinical gastric fluid samples incubated at 37 °C for 0, 0.5, 1, 2 and 3 h. Panels d and g created with BioRender.com.

Assembly of the electronic components into the capsule

Among orally administered detection platforms, electronic capsules offer a promising means for in situ analysis of DNA molecules within the gastrointestinal tract[32]. To achieve *in vivo* monitoring of pathogenic DNA in the stomach, the envisioned capsule shall capture pathogens via active inhalation and enable CRISPR/Cas-based DNA detection, demanding appropriate physical isolation and signal transduction interfaces. Among previously reported CRISPR-based systems, optical signals (including absorbance[33], colorimetric[34,35], fluorescence[36,37], and bioluminescence[38,39]) are most commonly employed owing to their favorable sensitivity. Thus, an efficient photosensor shall be integrated. Based on these considerations, we designed the overall capsule architecture (Figures 3a, S3a). It comprised a vacuum-driven sampling module and the sampling chamber consisted of an inner cavity A and an outer cavity B, each equipped with two independent inlet ports. Gastric fluid was firstly pumped into cavity A and subsequently transferred to be stored in cavity B, thereby achieving processing by CRISPR/Cas system (introduced

later) (Figures 3b, S3b). The fluidic and electronic regions were physically isolated to prevent liquid accidental leakage and electrical interference. The overall dimensions of the capsule were 35 mm × 14 mm, confirming its compatibility for swallowing and passing through whole digestive tract (Figure 3c).

We first verified the active sampling of the capsule and revealed that diameters of 4.3-4.4 mm facilitated effective liquid uptake (Figure S3c). The simulated gastric liquid spiked with dye was observed entering sampling cavity B within 5-8 s (Figures 3d, S3d, and Video S1), demonstrating the rapid sampling capability. To further validate *in vivo* feasibility, we placed the capsule in the canine stomach for *in vivo* sampling tests, confirming controllable gastric fluid collection (Figure 3e). We also validated the liquid-tight performance of the capsule. After complete immersion in deionized water for 24 h, the overall mass showed only a slight increase due to water absorption by the housing material or adhesives (Figure S3f). The visual inspection revealed no liquid intrusion into the internal electronic regions, indicating that the packaging effectively protected the internal electronics.

In addition, we verified the optoelectronic signal transduction capability. Here, an LED light source with certain wavelength was temporarily used to mimic CRISPR-derived luminescence signals. The light could be switched on and off via smartphone control, enabling real-time monitoring of the photosensor response through the recorded ADC values (Figures 3f, g, S3e, and Video S2). Meanwhile, after verification the capsule's wireless communication through porcine tissue *in vitro* (Figures S4a-c), we assessed its energy consumption. By recording current variations across different operational states (Broadcast mode, Bluetooth connection, sensing module activation, sampling module

activation, function shutdown, and return to Broadcast mode), we systematically analyzed the current-consumption profiles (Figure 3h). The results demonstrated that the capsule could achieve coordinated operations of electronic modules under constrained energy conditions.

Finally, the validation in canine stomach confirmed that the capsule could accomplish *in vivo* optoelectronic signal conversion and wireless monitoring (Figures 3i, j). The LED light was turned on and off via external control, and the real-time photosensor output signals could be read on smartphone. Additionally, the sampling and optoelectronic signal conversion were also validated in porcine model (Figures 3k, S5). Collectively, the ingestible electronic capsule achieved stable active sampling and optoelectronic signal transduction in both *in vitro* simulated environments and *in vivo* the animal stomachs, providing a reliable platform foundation for further integration of the CRISPR/Cas-based DNA-sensing system and *in vivo* detection.

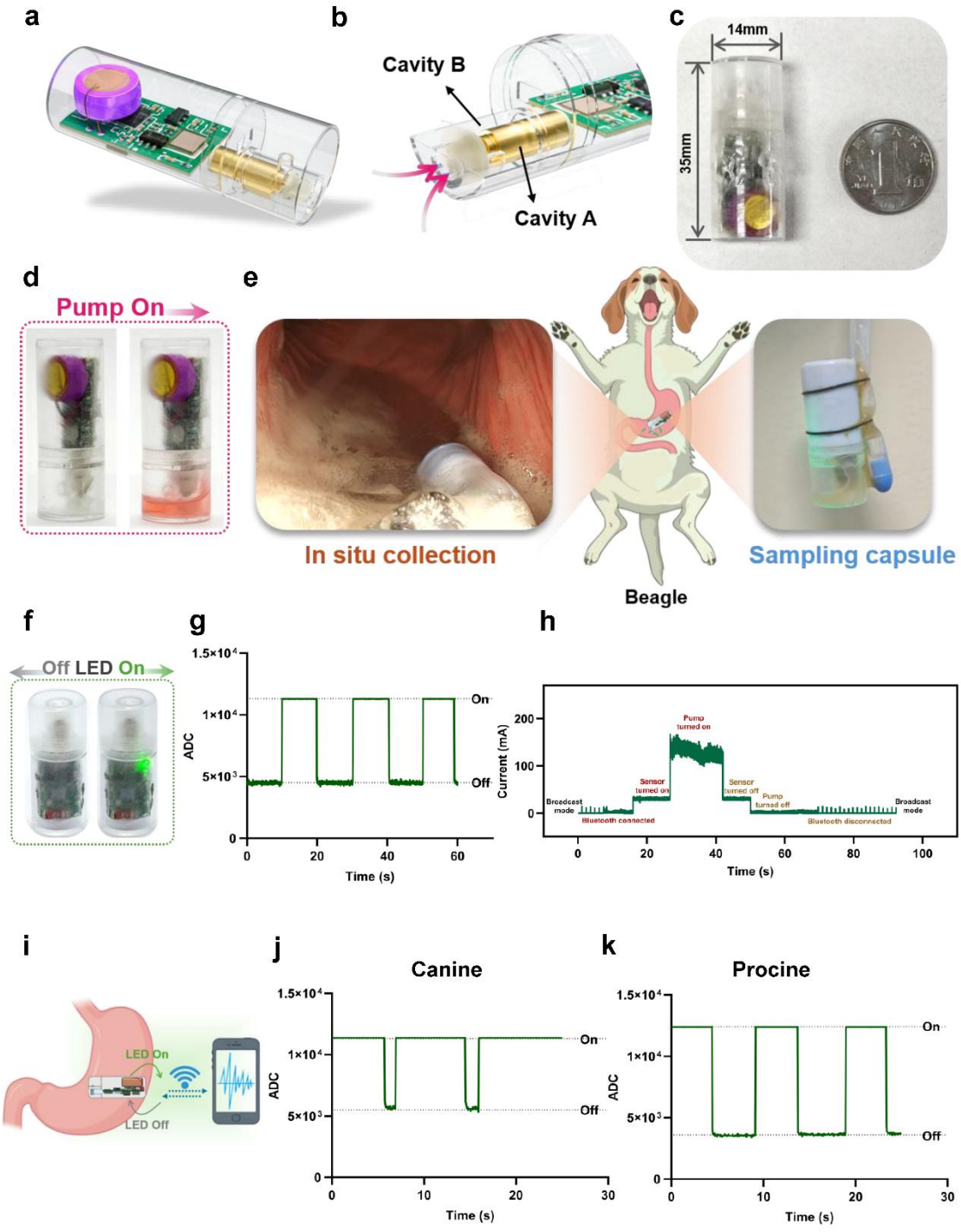


Figure 3. System design and functional validation of the electronic capsule. a, Three-dimensional schematic of the ingestible electronic capsule. **b**, Detailed view of the sampling chamber, showing the internal architecture for gastric fluid collection. **c**, Dimensions of the electronic capsule. **d**, Demonstration of the active sampling function of the electronic capsule (mm). **e**, In vivo gastric sampling in a dog. The left image shows endoscopic visualization of the capsule during gastric sampling, whereas the right image

shows the corresponding sampling process of the electronic capsule. **f**, Demonstration of the LED on–off control function of the electronic capsule. **g**, Photoelectronic responses of the electronic capsule under alternating LED "On-Off" states under strictly dark condition. **h**, Power consumption characterization of the electronic capsule under different operating modes. **i**, Schematic illustration of *in-vivo* sensing by the electronic capsule in the gastric environment. **j**, Sensing signal response of the electronic capsule in the stomach of a dog. **k**, Sensing signal response of the electronic capsule in porcine stomach.

Integration of paper-based CRISPR/Cas system into the capsule

The capsule was intentionally designed with dedicated space for the CRISPR/Cas system in cavity B and above the circuit board. The key challenge was to perform CRISPR/Cas multi-step reactions in this confined volume while generating an optical signal intense enough for the onboard photosensor. Absorbance and fluorescence modalities were ruled out due to requirement of bulky illumination or laser components. We therefore adopted bioluminescence via dual dCas9–sgRNA–mediated NanoLuc reconstitution to establish a CRISPR/dCas9 system[39]. After optimizing the system in a stepwise format, we primarily achieved significant bioluminescent output for detection of the *Salmonella invA* gene *in vitro* tubes (details shown in supplementary results and Figures S6a-h).

To enable multi-step CRISPR/dCas9 reactions (enrichment, lysis, amplification, and detection) within the confined capsule space, we adopted a stacked paper-based platform that leverages capillary wicking and PVA delay layers to segregate reaction zones, transport analytes, and regulate flow rates (Figure 4a). We integrated this paper-based format into the capsule (Figures 4b). where active sampling would deliver gastric fluid from cavity A to the paper absorption channel in cavity B. To facilitate loading, the overall paper dimensions were

designed as 10 mm × 10 mm, with a central reaction zone of 6 mm diameter and hydrophobic boundaries defined by wax printing to confine liquid diffusion (Figure 4c). To accommodate the timing requirements of multi-step reactions, we introduced 10% PVA delay layers (3 mm pore size) between different functional zones to regulate liquid migration velocity. Additionally, by comparing the liquid absorption capacities of the strips with varying lengths (1.0, 1.5, and 2.0 cm), we selected the 1.5 cm design, which exhibited a maximum absorption volume of approximately 150 μL (Figure S8a).

Following gastric sampling, the absorbed sample entered the pretreatment zone, where immobilized lysozyme (via Schiff base chemistry) locally lysed pathogenic bacteria to release nucleic acids without interfering with downstream RPA and CRISPR reactions (Figures S7a-c). Released nucleic acids then flowed into the RPA zone for target amplification, and the products moved to the dual dCas9–sgRNA detection zone, where target binding reconstituted and activated NanoLuc. Real-time recording of liquid migration across different zones confirmed that this multilayered paper-based architecture enabled sample transport and sequential reaction initiation (Figure S8b). Through coupling the bioluminescence zone of the paper-based sensor with the photosensor diode on the circuit board by a contactless way, optoelectronic signal transduction interface was established (Figure S9b, c).

Subsequently, we systematically evaluated the analytical performance of the integrated DNA-sensing capsule (Figures 4d, S9a-c). The output bioluminescent signals were measured using a microplate reader and analyzed in conjunction with the capsule, revealing a strong positive correlation among *Salmonella* concentration, luminescence intensity and photocurrents across the range of 10^2–10^8 CFU/mL detected strains (Figures 4e, f, S9d-f). To validate the

target specificity of the detection system, we separately assayed 1×10^4 CFU/mL of *Escherichia coli*, *Bacillus subtilis*, *Staphylococcus aureus*, and *Salmonella typhimurium*, proving that only the *Salmonella* group produced significantly positive detection signals (Figure 4g). To further simulate the complex microbial compositions, we mixed *S. typhimurium* with the above three non-target strains at varying proportions and performed detection. The results showed that as the proportion of *S. typhimurium* increased, the photocurrent signals output by the electronic capsule gradually intensified (Figure 4h), confirming that the system enabled quantitative detection of target pathogens against a complex microbial background. To sum up, we verified the capsule's performance for realizing CRISPR/Cas-based detection of target pathogen.

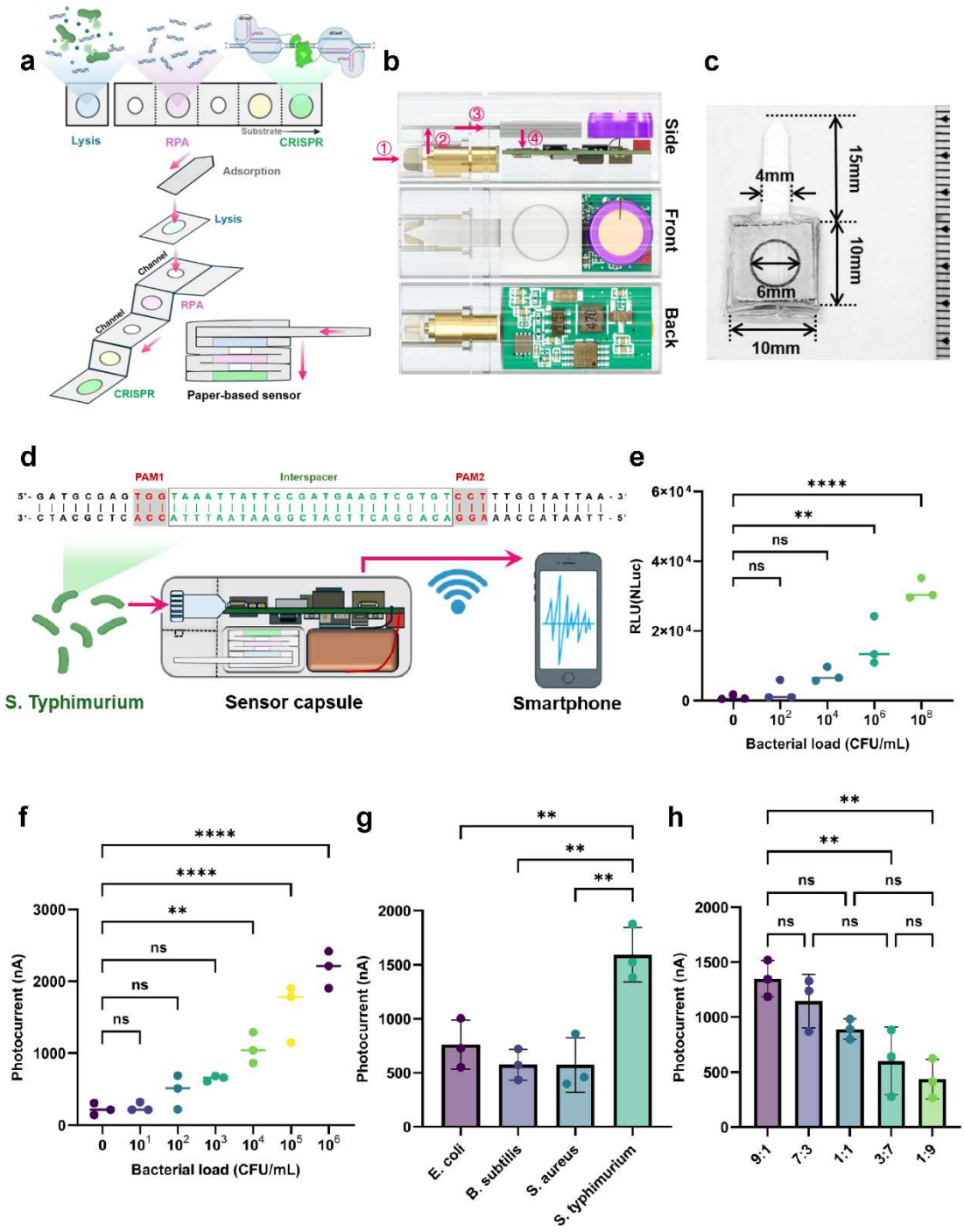


Figure 4. Integration of a paper-based nucleic acid sensor with an ingestible electronic capsule for pathogen detection. a, Structural design and working principle of the paper-based nucleic acid sensor. The upper panel illustrates the sensing principle, whereas the lower panel shows the unfolded and folded configurations of the sensor. Grey regions indicate hydrophobic barriers; blue, purple, yellow, green and white circles denote the lysis, RPA, chemiluminescent substrate, CRISPR detection and PVA delay regions,

respectively. Arrows indicate the direction of liquid flow. **b**, Three-dimensional schematic views of the integrated electronic capsule from the side, front and rear. The upper panel illustrates the capsule operation sequence from ① to ④. **c**, Dimensions of the paper-based nucleic acid sensor. **d**, Schematic illustration of sequence-specific detection of a Salmonella by the ingestible electronic capsule. Following intragastric sampling, the Salmonella is processed on a paper-based sensor for lysis, RPA amplification and sequence-specific detection, with the resulting signal wirelessly transmitted to a smartphone. **e**, Chemiluminescence intensity (NanoLuc, Nluc) generated by the paper-based sensor in response to different bacterial loads. **f**, Photocurrent responses of the electronic capsule to different bacterial loads in simulated gastric fluid. **g**, Specificity assessment of the electronic capsule in simulated gastric fluid. **h**, Photocurrent responses of the electronic capsule to different proportions of mixed bacterial populations in simulated gastric fluid.

In vivo test of the bioelectronic capsule on large animal models

To further investigate whether the integrated bioelectronic capsule could enable in situ analysis of DNA molecules in the gastric environment while preserving their biological information, we established canine and porcine models to evaluate its performance *in vivo* (Figure 5a). Beagle dogs or pigs were orally gavaged with 1×10^6 CFU/mL of an engineered *E. coli* MG1655 strain carrying a partial fragment of the *Salmonella invA* gene (Figure S10). PBS-gavaged animals served as negative controls. Following gavage, the capsule was guided into stomachs with the endoscopic assistance and activated for sampling and detection (Figures 5b, S11a-c).

Approximately 30 min after initiating *in-vivo* detection, the experimental canine group exhibited significantly higher photocurrents than the PBS control, confirming that the capsule effectively recognized *Salmonella invA* gene target

in the canine stomach (Figure 5c). Notably, photocurrent declined after 40 min, likely due to acid-induced impairment of enzyme activity in the paper-based sensor, despite prior $NaHCO_3$ neutralization. This observation underscored the need to optimize the gastric detection window coupled with reagent stability. To corroborate these results, we performed parallel *ex vivo* gastric fluid assays by collecting the samples at 0–40 min post-gavage and using the capsule (Video S3). Significant photocurrents at all time points indicated sustained bacterial presence over this window, whereas controls showed no specific signals (Figures 5d, S11d). The concordance confirmed the capsule's ability to capture transient nucleic acid signals *in vivo*. Notably, no target signals were detected in fecal samples within 24 h post-gavage (Figure S11e). A histological assessment of gastric tissues proved biosafety of loading capsule *in vivo* (Figures S11f, g).

In addition, pigs share high similarity with humans in gastrointestinal anatomy, physiology, and scale, making them valuable for evaluating the translational potential of *in-vivo* detection using our capsule. Following the similar gavage regimen, the capsule was placed in porcine stomach (Figures S12a, b, Video S4). At 80 min post-initiation, the experimental group showed markedly higher photocurrents than the PBS control (Figure 5e), confirming successful detection of target *Salmonella invA* gene in the porcine stomach. Concurrently, gastric fluid was collected at 0, 20, 40, 60, and 80 min post-gavage for *ex vivo* capsule testing. Only experimental group samples yielded positive photocurrent responses (Figure S12c), with an evident signal decay trend over time (Figure 5f). These results corroborated the *in-vivo* findings and confirmed gastric persistence of the target pathogen, while fecal samples remained negative for detectable signals (Figure 5g). Biosafety assessment of serum SAA and IL-6 levels before and after capsule deployment along with PBS or strains revealed no elevation difference, indicating no capsule-induced inflammatory response

(Figures S12d, e).

Collectively, *in vivo* validation in canine and porcine models confirmed that the capsule enables gastric sampling, nucleic acid recognition, and wireless electronic readout. The system performed molecular detection directly within the stomach, marking a critical advancement from *ex vivo* sampling & detection to *in vivo* sampling & detection. This capability circumvented the time delays inherent in conventional fecal testing caused by bacterial migration, colonization, and excretion, enabling direct capture of transient gastric nucleic acid signals and providing a new approach for early, dynamic monitoring of gastrointestinal infections.

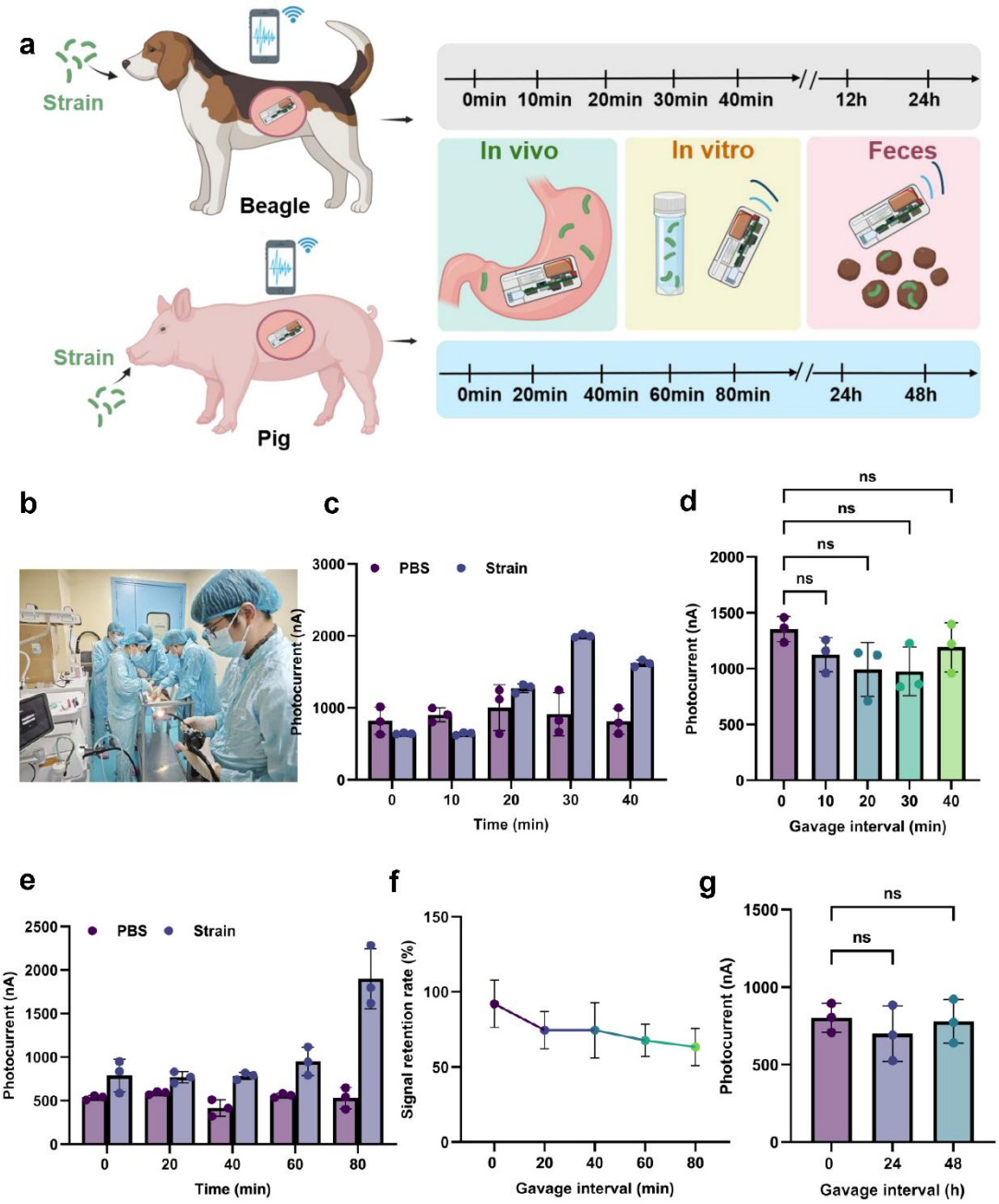


Figure 5. In vivo validation of the ingestible electronic capsule in large-animal models. a, Schematic illustration of the experimental workflow for evaluating the ingestible electronic capsule in large-animal models. **b**, Photographs showing the experimental procedure in the canine model. **c**, Electronic capsule signal recorded in the canine stomach at 0, 10, 20, 30 and 40 min after oral gavage. **d**, Photocurrent signals recorded *ex vivo* from the electronic capsule following gastric sampling at 0, 10, 20, 30 and 40 min after oral gavage in dogs. **e**, Photocurrent responses of the *in vivo* electronic capsule recorded at 0, 20, 40, 60 and 80 min after oral administration. **f**, Comparison of sample signal retention

between *ex vivo* and *in vivo* measurements using the electronic capsule. **g**, Photocurrent signals measured from faecal samples collected before and at 24 and 48 h after oral gavage. Panel a created with BioRender.com.

Application of the bioelectronic capsule for clinical sample detection

In order to advance our bioelectronic capsule toward clinical translation, we addressed the safe retrieval of capsule by incorporating a tethered design, allowing active removal after detection to reduce gastrointestinal retention and enhance controllability. This approach was validated in a porcine model given its similarity to the human digestive tract (Figure 6a). A food-grade silicone sheath was added to minimize mucosal irritation (Figure 6b), and successful retrieval confirmed feasibility (Figure 6c and Video S5), establishing a workflow of ingestion, DNA detection, and tethered extraction (Figure 6d). This configuration transforms the capsule into an intragastric diagnostic platform with controlled entry, active sampling, detection, and active retrieval, reinforcing safety for future clinical use.

To further pave the way toward practical implementation, we employed clinical gastric fluid samples to validate the molecular detection capability of this platform. Given that *Helicobacter pylori* was a common gastric pathogen closely associated with various gastric disorders[40], we designed a *H. pylori* 16S rRNA detection system (Figure S13) and tested it on gastric fluid samples collected from 15 volunteers (9 males, 6 females, aged 18-60; Figure 6e) with biosafe gastric juice collection tubes. Initial urea breath testing identified 4 positive and 11 negative cases, while qPCR on gastric fluids yielded 12 positive and 3 negative results. The observed discrepancies underscored the need for *in vivo* nucleic acid detection. The *ex vivo* capsule-based testing produced significant photocurrent responses in four samples, which were also positive by both

breath test and qPCR (#5, #6, #7, #10; Figures 6f, S14a, b), demonstrating concordance with established methods and supporting the platform's clinical feasibility. From these results, it was also evident that there was still considerable room for improvement in the sensitive detection techniques applicable to low-concentration samples.

Given the acidic, enzyme-rich gastric environment, we assessed nucleic acid degradation during *ex vivo* storage and the impact of this factor on capsule detection performance. Testing clinical samples after varying incubation times revealed that photocurrent in positive cases progressively declined with prolonged storage, confirming that target stability directly affects detection signals (Figure 6g). Negative samples remained unchanged, excluding nonspecific signal drift. This finding supported the capsule's advantage for immediate on-site detection, minimizing degradation-related information loss.

Finally, we evaluated manufacturing feasibility by establishing standardized assembly protocols for the capsule structure, paper-based sensor, and electronics, achieving small-batch fabrication under laboratory conditions (Figure S15). In summary, through tethered retrieval, clinical sample testing, stability assessment, and small-batch manufacturing, we systematically evaluated the capsule's translational potential across safety, clinical relevance, reliability, and scalability. Our study established a complete workflow from ingestion to *in-vivo* detection to active retrieval, providing a preliminary foundation for clinical translation of ingestible intragastric molecular diagnostic devices.

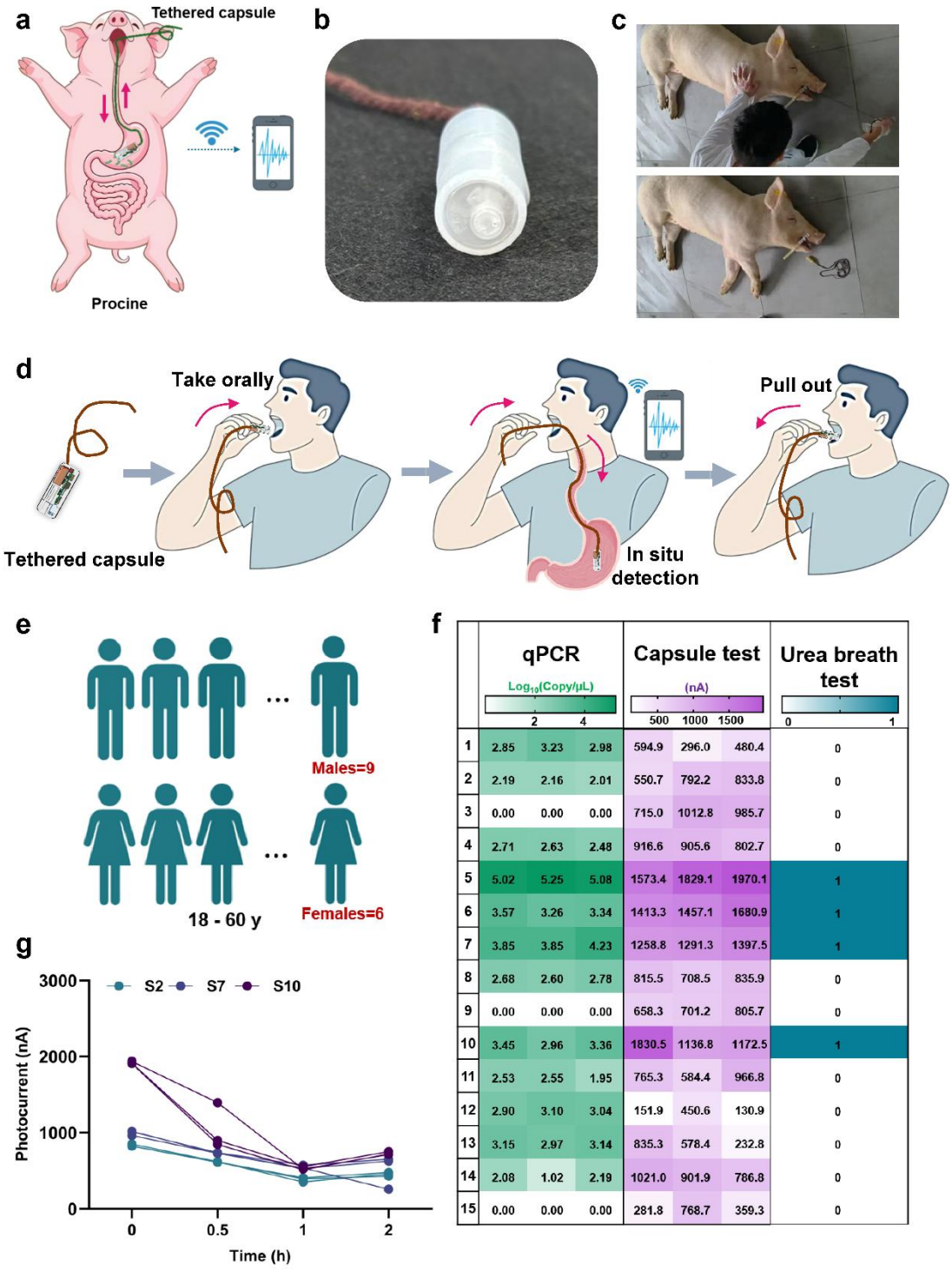


Figure 6. Retrieval and clinical validation of the tethered electronic capsule. a, Schematic illustration of the tethered electronic capsule for *in vivo* detection in pigs. **b**, Photograph of the electronic capsule equipped with a silicone protective sleeve. **c**, Photographs showing the tethered electronic capsule during *in vivo* detection and retrieval in a pig. **d**, Schematic illustration of the workflow for oral ingestion, *in vivo* detection and

retrieval of the tethered electronic capsule in humans. **e**, Schematic illustration of the clinical ^{13}C-urea breath test for *H. pylori* detection. **f**, Statistical comparison of qPCR, electronic capsule and breath-test results across 15 clinical samples. qPCR Ct values are shown as a white-to-green heatmap; electronic capsule photocurrent signals as a white-to-purple heatmap; and clinical breath-test results as white (0, negative) and blue (1, positive). **g**, Photocurrent responses of the electronic capsule to freshly collected clinical gastric fluid samples incubated at 37 °C for 0, 20, 40 and 60 min. Panels a and e created with BioRender.com.

Conclusion

In this study, we have developed an ingestible bioelectronic capsule integrating active sampling, paper-based microfluidic processing, CRISPR/dCas9-mediated DNA recognition, and wireless readout for *in vivo* detection of pathogenic DNA within the gastric environment. Validated *in vitro*, *ex vivo*, and *in vivo* canine and porcine models, it reliably captures transient nucleic acid signals otherwise lost to rapid clearance and degradation. Notably, the system achieved concordant results with qPCR and breath tests on patient samples, and its tethered design enables safe retrieval, supporting clinical translation.

Nevertheless, several limitations exist. First, the current detection window is constrained under gastric conditions, as evidenced by signal attenuation beyond 40 minutes *in vivo*. Although acid neutralization was applied, prolonged exposure remains challenging and necessitates further optimization of reagent formulations or protective matrices. Second, the paper-based sensor, while advantageous for simplicity and cost-effectiveness, may introduce batch-to-batch variability and affect reproducibility. Besides, paper-based structure limits multiplexing capacity and demands next-version design. Third, the current reliance on nucleic acid amplification (RPA) prior to CRISPR recognition adds

complexity to the workflow. Future iterations could explore amplification-free CRISPR-based detection to simplify the device and workflow.

Looking forward, this platform opens several promising avenues. The modular architecture allows facile adaptation to different pathogens by simply reprogramming sgRNA sequences, making it suitable for detecting antibiotic resistance markers[41], viral nucleic acids[42], or even tumor-associated DNA mutations[43]. Moreover, as CRISPR-based technologies continue to advance, the integration of high-fidelity Cas variants with enhanced target discrimination could extend the capsule's utility to single-nucleotide polymorphism (SNP) detection[44], enabling precise identification of drug-resistant strains (e.g. *H. pylori*) or cancer-related point mutations directly within the gastric environment. Combining additional sensors (pH[25,45-47], temperature[48], gastric electrophysiology[20], or biochemical markers[22,23]) could comprehensive gastrointestinal assessment. In parallel, advances in enzyme engineering[49], lyophilization[50], and encapsulation strategies could prolong reagent stability, while biocompatible materials could improve safety and patient compliance. With continued optimization, this intelligent capsule system represents a paradigm shift from *ex vivo* testing to *in vivo* real-time molecular diagnostics, facilitating early disease detection, personalized monitoring, and timely intervention for gastrointestinal disorders.

Methods

Plasmid construction, protein expression and purification

Two recombinant plasmids of pET28a-dCas9-LgBiT-6×His and pET28a-dCas9-SmBiT-6×His were synthesized by Angsheng Life Science and Technology Co., Ltd. The protein sequences were summarized in Table S1. The

constructed plasmids were directly transformed into *E. coli* Shuffle T7-B competent cells (ZC1229, ZOMANBIO) for expression of dCas9-LgBiT-His and dCas9-SmBiT-His proteins, respectively. Transformed strains were cultured in Luria-Bertani (LB) medium containing kanamycin (50 μg/mL) (25389-94-0, HEOMNS) at 37 °C with shaking at 200 rpm until the OD_{600} reached 0.4–0.6. Protein expression was induced with 0.2 M isopropyl β-D-1-thiogalactopyranoside (IPTG, 367-93-1, HEOMNS). The cultures were further incubated at 16 °C with shaking at 200 rpm for 16-18 h. Cells were harvested by centrifugation at 6,000 × g for 10 min, resuspended in equilibration buffer (50 mM NaCl, 1 mM TCEP, 20 mM HEPES, pH 7.4), and centrifuged again at 6,000 × g for 10 min. The pellet was resuspended in 30 mL of buffer and disrupted by ultrasonication. The lysate was centrifuged at 12,000 × g for 1 h, and the supernatant was filtered through a 0.22 μm membrane (YA0662, Solarbio). The supernatant was then purified using a Ni^{2+}-charged affinity column (05893682001, Roche), and bound proteins were eluted with elution buffer (50 mM NaCl, 1 mM TCEP, 20 mM HEPES, 10% glycerol, 40 mM imidazole, pH 7.4). The eluted proteins were concentrated and buffer-exchanged into PBS (pH 7.2-7.4, P1012, Solarbio) using 100 kDa ultrafiltration tubes (UFC910096, Millipore). Following concentration, the samples were further purified by size-exclusion chromatography on a Superdex 200 Increase 10/300 GL column (28990944, Cytiva). Target protein fractions were collected based on chromatographic profiles, concentrated using 100 kDa ultrafiltration tubes, and quantified using a BCA assay kit (WB6501, NCM Biotech).

DNA degradation validation in simulated gastric fluid

To evaluate the degradation kinetics of DNA fragments in simulated gastric fluid, the linearized DNA or circular plasmids containing the *invA* gene were added to tubes containing simulated gastric fluid to final concentrations of 10 nM or 100 nM. The mixtures were gently mixed and incubated at 37 °C. Samples were

withdrawn at 0, 0.5, 1, 2, and 3 h post-incubation and immediately placed on ice to terminate the enzymatic reaction. Residual invA gene fragments in the samples at each time point were quantified by qPCR. Each concentration group consisted of three parallel samples, and each qPCR reaction was performed in duplicate. The experiment was independently repeated three times, and results were expressed as mean ± SD.

Dual dCas9-sgRNA assay for nucleic acid detection

Guide RNAs (sgRNAs) targeting the *Salmonella invA* gene were designed using the online tool CRISPOR developed by Haeussler et al. The sequences are listed in Table S3 and were synthesized by Angsheng Life Science and Technology Co., Ltd. The synthesized sgRNA pellets were dissolved in IDTE (IDT nuclease-free duplex buffer) and stored for subsequent use. Pre-assembly of ribonucleoprotein (RNP) complexes was performed in a reaction mixture containing 2 μM dCas9-LgBiT-His or 2 μM dCas9-SmBiT-His protein, 7.5 μM sgRNA, and reaction buffer composed of 20 mM Tris-HCl (pH 7.5), 150 mM KCl, 5 mM $MgCl_2$, 5% (v/v) glycerol, 1 mM DTT, and 1 mg/mL BSA. The mixture was incubated at 37 °C for 20 min to form dCas9-Lg:gRNA1 and dCas9-Sm:gRNA2 RNP complexes, respectively, which were then stored at −80 °C until use. For detection, 5 μL of each RNP complex was added to a reaction buffer containing 20 mM Tris-HCl (pH 7.5), 150 mM KCl, 5 mM $MgCl_2$, 5% (v/v) glycerol, 1 mM DTT, and 1 mg/mL BSA to a final volume of 19 μL. Subsequently, 1 μL of the target nucleic acid fragment was added, mixed thoroughly, and incubated at 37 °C for 30 min. After the reaction, signals were read using a microplate reader (VICTOR Nivo™, Revvity) for luminescence intensity, or chemiluminescence images were captured using an imaging system (Tanon-5200) for result interpretation.

Target DNA-dCas9-sgRNA binding validation

In a reaction buffer (20 mM Tris-HCl pH 7.5, 150 mM KCl, 5 mM $MgCl_2$, 5% (v/v) glycerol, 1 mM DTT, 1 mg/mL BSA), 50 nM of target or non-target DNA fragments were incubated with 0, 50, 200, or 800 nM of dCas9-Lg:gRNA1, dCas9-Sm:gRNA2, or both complexes combined, at room temperature for 1 h. Prior to electrophoresis, 6× loading buffer (BM111-01, TRANSGEN) was added to the reaction mixtures, and samples were loaded onto a 2% agarose gel. Electrophoresis was performed in TAE buffer (T1060, Solarbio) at a constant voltage of 150 V for 15 min. Bands were visualized and photographed using a chemiluminescence imaging system (UVITEC).

Paper-based DNA sensor fabrication

Whatman Grade 1 chromatographic cellulose paper (3001-861, GE Healthcare) was used as the substrate for paper-based device fabrication. The device comprised three independent functional modules: sample lysis pretreatment, RPA isothermal amplification, and dual dCas9-CRISPR detection. Each reaction zone was designed as a circular area of 6 mm in diameter. Modules were interconnected by delay layers of 3 mm in diameter, fabricated from 10% (w/v) polyvinyl alcohol (PVA, type 1799) (P815725, MACKLIN). Except for the reaction zones and delay layers, the remaining hydrophobic areas of the paper were coated with molten paraffin wax, which was then fully permeated by heating to create hydrophobic barriers.

For lysozyme immobilization in the sample pretreatment module, paper discs were soaked in 0.1 mol/L sodium periodate (7790-28-5, Aladdin) solution and incubated at room temperature in the dark for 60 min. After washing with ultrapure water (ddH_2O), the discs were transferred to 2 mg/mL lysozyme

solution (pH 7.4) and incubated at 4 °C for 4 h, followed by incubation in 1 mg/mL sodium cyanoborohydride (2895-60-7, Leyan) for 30 min. Finally, the discs were blocked with 1% (w/v) bovine serum albumin (BSA), lyophilized, and stored at −20 °C until use. The RPA module utilized lyophilized components from a commercial kit (BA-LYO-96, EZassay), with primer sequences listed in Table S2. The lyoprotectant formulation for CRISPR protein components consisted of 1% BSA, 10% trehalose (99-20-7, HEOMNS), and 10% sucrose (w/v) (57-50-1, HEOMNS). A 20 μL aliquot of the mixture was lyophilized overnight in a freeze dryer and stored at −80 °C.

The three functional modules (pretreatment, RPA, and detection) were placed on a clean workbench. Corresponding volumes of reaction reagents were dispensed onto each circular reaction zone and air-dried at 37 °C, followed by addition of lyophilized components to the respective modules. The modules were then arranged in sequence according to sample flow direction (from pretreatment to RPA and detection), and the trailing edges of the delay layers were serially connected using absorbent paper strips (fibrous absorbent filter paper), enabling sequential directional liquid transport under capillary action. To ensure intimate contact and smooth liquid transfer, the assembled device was gently pressed and fixed. Finally, the entire paper-based device was completely encapsulated with transparent adhesive tape (3M), and stored at −80 °C in the dark until use.

Electronic capsule assembly

The capsule housing was fabricated using 3D printing technology with photosensitive transparent resin (Yixin 3D, Beijing). The housing comprised two independent compartments. A first compartment was designed as a dual-chamber structure, containing an inner sampling cavity A and an outer cavity B.

The cavity A served for pump-driven sampling and cavity B served for absorption of samples on paper-based fabrication. The second compartment accommodated the Bluetooth signal transmission circuit board, micro-battery, and paper-based detection chip. A transparent partition, also 3D-printed, was positioned between two compartments and fitted into the fixing slot of the micro-peristaltic pump during assembly. It was worth noting that the most paper fabrications except for absorption part were located in the second compartment with strict sealing nearby photosensor. This was set for establishing optical-electronic signal conversion interface. The whole compartmentation design served to physically isolate the liquid sample from all electronic components, thereby preventing liquid ingress that could cause short circuits or signal interference.

Prior to assembly, all visible gaps were coated and sealed with medical-grade acrylic adhesive (3321, LOCTITE). After adhesive application, UV irradiation at 365 nm for 5 s was applied to accelerate curing and form a dense sealing layer. Subsequently, two compartments were aligned and pressed together via the snap-fit structure, and a uniform layer of adhesive was applied around the joint to ensure complete coverage of all mating interfaces, followed by a second UV irradiation at 365 nm for 5 s to fully cure the adhesive. All operations were performed within a clean bench.

Capsule power consumption measurement

To evaluate the power consumption characteristics of the built-in circuit system under different operating modes, a digital source meter was connected to the power supply input terminals of the capsule circuit board to monitor current variations throughout the entire workflow in real time. The source meter was set to the rated operating voltage of the battery, with current range set to auto-

ranging and a sampling frequency of 10 Hz to capture transient current changes. The test sequence was performed as follows: (1) Bluetooth module was activated to establish connection with the smartphone APP, and the standby current after stable connection was recorded; (2) the sensor module was turned on and the operating current was recorded; (3) the micropump was started, and both the instantaneous peak current and stable running current were recorded; (4) the sensor module was turned off and the current decay was observed; (5) the micropump was turned off and the post-stop current was recorded; (6) the Bluetooth connection was disconnected and the final standby current was recorded. Throughout the entire test, the source meter continuously recorded the current-time curve.

Photosensing assessment in capsule

To evaluate the signal response characteristics of the built-in photosensor within a light-tight environment, a black light-tight test box (Qingxinrui Electrostatic Protection Technology Co., Ltd.) was used as the test chamber to exclude external ambient light interference. The assembled capsule was placed at the center of the test box, and the lid was closed to ensure complete darkness. The Bluetooth module was connected via the smartphone APP, and after stable connection, the sensor module was activated to initiate continuous ambient light intensity signal acquisition. After stable sensor operation for 10 s, the LED light source on the circuit board was triggered remotely via the APP to illuminate for 10 s, followed by shutdown, constituting one complete cycle. This procedure was repeated for three cycles (LED on-off), with each on/off action synchronized by control commands sent from the APP to ensure timing consistency. Throughout the test, the APP continuously received and recorded the ADC values (digital units, corresponding to relative light intensity) output by the sensor.

Kinetics of capsule detection

Salmonella enterica subsp. enterica serovar Typhimurium strain CDC 6516-60 (ATCC 14028) was used as the model strain. The signal response kinetics of the capsule were evaluated and the signal plateau phase was determined. *Salmonella* was inoculated into appropriate liquid medium and cultured overnight at 37 °C with shaking at 220 rpm to stationary phase. The initial viable concentration of the overnight culture was determined by plate counting, and the culture was diluted with sterile PBS buffer (pH 7.4) to 1×10^4 CFU/mL. Ten fully assembled paper-based capsules were labeled #1 through #10, and samples were collected via the capsule sampling mechanism. After sampling, the capsules were allowed to react at room temperature, and signals were collected at 0, 20, 40, 60, and 80 min. At each time point, the Bluetooth connection was established via the smartphone APP, the sensor module was activated, and the chemiluminescent signal (ADC value) from the paper-based detection zone was read. Each capsule was read three times consecutively, and the average value was taken as the signal value at that time point.

DNA-monitoring sensitivity of the capsule in simulated gastric fluid

To evaluate the quantitative detection capability of the capsule sensor for varying concentrations of *Salmonella*, a series of bacterial suspensions were prepared using simulated gastric fluid (R22733, Yuanye) as the diluent. A single colony of *Salmonella* was inoculated into liquid medium and cultured overnight at 37 °C with shaking at 220 rpm to stationary phase. The initial viable concentration was determined by plate counting, and the culture was serially diluted 10-fold with simulated gastric fluid to prepare suspensions at concentrations of 1×10^1, 1×10^2, 1×10^3, 1×10^4, 1×10^5, and 1×10^6 CFU/mL, with simulated gastric fluid alone (0 CFU/mL) serving as the blank control. Each

concentration was injected into the sampling port of the capsule, with three parallel samples per concentration. After sample loading, the capsules were incubated at 37 °C for 1 h under static conditions. Following incubation, the Bluetooth connection was established via the dedicated smartphone APP, the sensor module was activated, and the ADC_{count} values corresponding to the chemiluminescent signals from the paper-based detection zone were recorded. Each capsule was read three times consecutively after signal stabilization, and the arithmetic mean was calculated. Background signal values (ADC_{count_0}) were also recorded, and the photocurrent value for each sample was calculated according to Formula 1. The experiment was independently repeated three times, and results were expressed as mean ± standard deviation (SD).

DNA-monitoring specificity of the capsule in simulated gastric fluid

To verify the specificity of the detection system, *Salmonella*, *Bacillus subtilis* BS168, Escherichia coli DH5α, and Staphylococcus aureus were individually diluted to 1 × 10^4 CFU/mL in simulated gastric fluid. These strains were tested individually, and additionally, Salmonella was mixed with each non-target strain at various volume ratios (9:1, 7:3, 1:1, 3:7, 1:9) to prepare a series of mixed bacterial suspensions. All samples were subjected to sampling, reaction, and signal reading following the same procedure described above.

In Vivo animal experiments

Ethics statement and animal models. Male C57BL/6 mice (6–8 weeks old; purchased from Tianjin Guosheng Zhongyuan Co., Ltd.) were used for the mouse experiments, which were approved by the Institutional Animal Care and Use Committee of Tianjin University (approval No. TJUE-2021-009). Male Beagle dogs (7–8 months old, weighing 10–12 kg; purchased from Nanjing

Chaimen Biotechnology Co., Ltd.) were used for the *in vivo* validation experiments, which were approved by the Institutional Animal Care and Use Committee of the School of Pharmaceutical Sciences, Hainan University (approval No. HPIACUC2026037). Male domestic pigs (weighing 30–50 kg; purchased from Yangwang Livestock Co., Ltd., Yongding District, Longyan) were used for the *in vivo* validation experiments, which were approved by the Institutional Animal Care and Use Committee of the School of Life Sciences, Longyan University (approval No. IRB-LYUN-2026-002L). All animal experiments were conducted in strict accordance with the Guide for the Care and Use of Laboratory Animals. Animals were acclimatized for 1 week under standard conditions (temperature 22 ± 2 °C, humidity 50%-60%, 12 h light/dark cycle) prior to experiments.

Detection of bacterial DNA residue in mouse stomach and feces. The invA-integrated MG1655 strain was inoculated into appropriate liquid medium and cultured overnight at 37 °C with shaking at 220 rpm to stationary phase. The initial viable concentration of the overnight culture was determined by plate counting, and the culture was diluted with sterile PBS to concentrations of 1×10^2, 1×10^3, and 1×10^4 CFU/mL, with PBS alone serving as the control. Mice were divided into 16 groups (n = 4 per group) and administered 100 μL of bacterial suspension or PBS by oral gavage. Gastric tissues were collected prior to gavage and at 0.5, 1, 1.5, and 2 h post-gavage. The stomachs were lavaged with 500 μL of PBS, and the gastric lavage fluid was collected for subsequent qPCR analysis. Fecal samples were collected prior to gavage and at 0.5 h intervals thereafter. Fecal samples were homogenized with 500 μL of PBS, heated at 99 °C for 5 min, centrifuged, and the supernatants were collected as templates for qPCR analysis.

One microliter of gastric lavage fluid or fecal supernatant was added to the qPCR reaction mixture and amplified under the same qPCR reaction conditions described above. A standard curve was established with $\log_{10}$(bacterial load) (CFU/mL) on the X-axis and corresponding Ct values on the Y-axis. The regression equation was fitted and the correlation coefficient was calculated (R^2 = 0.9331). The Ct values of samples at each time point were substituted into the standard curve equation (Formula 2) to estimate the bacterial load (CFU/mL) in each sample. Formula 2: $Y = -(X - 27.791) / 1.9013$

Preoperative preparation and anesthesia. Animals were fasted for 12 h and deprived of water for 4 h before experiments. To eliminate the interference of gastric acid on sensor signals, omeprazole (1 mg/kg) was administered orally one day prior to the procedure, and gastric acid was neutralized by intragastric administration of 5% sterile sodium bicarbonate solution (5 mL/kg) immediately before the operation. Anesthesia protocols varied by species: dogs were induced with Zoletil 50 (5 mg/kg) in combination with atropine sulfate (0.05 mg/kg) via intramuscular injection; pigs were induced with ketamine (10 mg/kg) combined with xylazine (1 mg/kg) via intramuscular injection. After loss of corneal reflexes and muscle relaxation, animals were fixed in left lateral recumbency, and an oral speculum was placed to expose the esophageal opening.

Sampling procedure and sensing function validation. The encapsulated capsule was orally delivered into the stomach and fixed in place. After Bluetooth connection via the dedicated smartphone APP, the following operations were performed sequentially: (1) The sampling switch was activated for 5-8 s to allow gastric fluid to enter the paper-based reaction zone; the capsule was then retrieved by traction, and the sampling area was photographed for

documentation; (2) The built-in LED light source was alternately turned on and off, and ADC signals were continuously recorded for 25 s to evaluate the dynamic sensor response. This procedure was strictly consistent across all individual animals.

Infection model establishment and dynamic monitoring. Following the basic functional validation, The E. coli MG1655 with *invA* integration (resuspended in sterile PBS) was administered by oral gavage. The dosage was adjusted according to species (1 mL for dogs, 50 mL for pigs), with a final concentration of 1×10^6 CFU/mL in both cases. Control animals received an equal volume of sterile PBS. In vivo photocurrent signals were recorded at multiple time points before (0 min) and after gavage (dogs: 10, 20, 30, 40 min; pigs: 20, 40, 60, 80 min). At each time point, gastric fluid samples were collected simultaneously via gastric tube (1–2 mL for dogs, 5–10 mL for pigs). A portion of each sample was used for *ex vivo* capsule testing, and the remainder was aliquoted and stored at –20 °C for subsequent qPCR template preparation.

Fecal sample processing and detection. Fecal samples were collected before (0 h) and at designated intervals after gavage (dogs: 12 h, 24 h; pigs: 24 h, 48 h). One gram of feces was weighed and homogenized with 1 mL of sterile PBS by vortexing. The homogenate was heated at 99 °C in a metal bath for 5 min to lyse cells and release DNA, followed by centrifugation at 12,000 × g for 10 min. The supernatant was collected as the qPCR template and also used for photocurrent signal detection by the electronic capsule. Gastric fluid samples were subjected to the same heat treatment, and the supernatants were stored together with fecal supernatants at -80 °C for further analysis. All procedures were performed under strict aseptic conditions. Measurements at each time point were performed in triplicate, and data were expressed as mean ± SD.

Human ethics and consent to participate declarations

This study recruited 15 volunteers aged 18-60 years. The protocol was approved by the Ethics Committee of Shanghai Changhai Hospital (approval No. CHEC2023-213). All participants were informed that the study procedure involved obtaining gastric fluid samples solely through maure clinical sampling methods. The subsequent sample processing through this study's methods did not involve in vivo experimentation. All participants also accepted the safety risks associated with relevant research.

Consent to publish declaration

All participants were informed of and consented to the fact that the data obtained from their clinical samples, after processing according to the methods described in this study, will be presented in this article in non-identifying form.

Clinical sample detection

All 15 human volunteers fasted for at least 4 h (both food and water) prior to sample collection, and gastric fluid samples were collected after obtaining informed consent. Gastric fluid samples were collected from these 15 volunteers using gastric fluid collection tubes. After collection, samples were neutralized and used for subsequent nucleic acid detection and electronic capsule testing.

For qPCR detection, 1 μL of gastric fluid sample was used as the PCR template. Detection of Helicobacter pylori was performed using a probe-based fluorescence qPCR kit (BES231115P, BIOESN) according to the manufacturer's

instructions. Results were interpreted as positive or negative based on the kit's criteria. Concurrently, all volunteers underwent clinical urea breath testing, with results interpreted according to standard clinical criteria.

Clinical gastric juice sampling was performed using a biosafety sampling tube. For electronic capsule testing, approximately 150 μL of neutralized gastric fluid sample was loaded into the sampling module of the electronic capsule. The integrated paper-based nucleic acid sensor completed sample processing, RPA amplification, and CRISPR-mediated detection, and the photocurrent signals output by the electronic capsule were recorded. The consistency of results among the three methods (qPCR, urea breath test, and electronic capsule) was evaluated.

To further assess the stability of target nucleic acids in gastric fluid and the effect of delayed detection, two independent experiments were performed. For qPCR analysis, clinically confirmed *H. pylori*-positive gastric fluid samples were collected and incubated at 37 °C. Aliquots were collected after 0, 1, 2 and 3 h of incubation and subjected to qPCR analysis. In a separate experiment, gastric fluid samples from an independent cohort were incubated at 37 °C for 0, 1 and 2 h, followed by electronic capsule testing. The photocurrent responses were recorded at each time point to evaluate changes in the target signal during sample incubation.

Data and code availability

The source data of the manuscript can be found at web links for publicly available dataset Figshare. This study does not report original code.

Acknowledgements

The authors thank for the support from the Testing Center in Hainan Engineering Research Center for Drug Screening and Evaluation, School of Pharmaceutical Sciences in Hainan University in this work. This work is supported by the following fundings: National Natural Science Foundation of China (32571637); Key Research and Development Program of Hainan Province (ZDYF2026GXJS003); Tianjin Natural Science Foundation for Distinguished Young Scholars (23JCJQJC00210); Beijing-Tianjin-Hebei Basic Research Cooperation Project of Beijing Natural Science Foundation (23JCZXJC00370); Shanghai “Pioneer Program” Bio-Hybrid Robot Project (25XF3200800); The Open Fund Project of State Key Laboratory of Synthetic Biology (HSK202601).

Author contributions

G.B., X.H., and X.L. conceived and designed the research. X.H. designed and tested the electronics. G.B. and X.L. designed, tested, and validated both the paper-based sensors and the integrated capsules. Y.B. and H.L. (Hui Liu) performed the animal experiments. H.L. (Hongxiang Li) assisted with the integration of the capsule systems and the design of the animal experiments. L.W. and X.C. prepared and validated the protein and CRISPR systems. M.Y., Z.B., X.T. and M.S. assisted with the in vivo validation of canine. J.C., J.L. and Y.Z. (Yi Zhang) assisted with the in vivo validation of porcine. Y.Z. (Yanning Zhang) and L.L. assisted with the generation of the schematic diagrams. H.Z. and Z.Y. assisted with the maintenance of the electronic components. Y.J., C.Z. and D.S. contributed to the generation of the engineered strains. X.J. helped with the collection of clinical samples. Y.W., H.Y. and T.H. assisted with the preparation of the paper-based sensors. G.B., C.H., Z.F. and D.L. wrote and revised the manuscript. H.W. designed the overall research framework and

supervised the project. All authors reviewed and approved the final manuscript.

Declaration of competing interest

The authors declare that they have no known competing financial interests or personal relationships that could have appeared to influence the work reported in this paper.

Supplementary Information

Supplementary information includes supplementary results, supplementary methods, supplementary figures of S1-S15, supplementary tables of S1-S4, and supplementary videos of S1-S5.

References

1 Jonaitis, P., Kiudelis, V., Streleckiene, G. *et al.* Novel Biomarkers in the Diagnosis of Benign and Malignant Gastrointestinal Diseases. *Dig. Dis.* **40**, 1-13 (2022).

2 Yang, Y., Ren, Y., Ma, T. *et al.* Research advances in the role of circulating microorganisms in gastrointestinal tumors (Review). *Mol. Clin. Oncol.* **24**, 40 (2026).

3 Zhang, R., Nie, Y., Chen, X. *et al.* A multicenter prospective clinical trial reveals cell-free DNA methylation markers for early esophageal cancer. *J. Clin. Invest.* **135**, 1558-8238 (2025).

4 Oh, T. J., Oh, H. I., Seo, Y. Y. *et al.* Feasibility of quantifying SDC2 methylation in stool DNA for early detection of colorectal cancer. *Clin. Epigenet.* **9**, 126 (2017).

5 Liu, Y., Zhang, Y., Dong, P. *et al.* Digestion of Nucleic Acids Starts in the Stomach. *Sci. Rep.* **5**, 11936 (2015).

6 Zhang, Y., Li, C., Liu, Y. *et al.* Mechanism of extraordinary DNA digestion by pepsin. *Biochem. Biophys. Res. Commun.* **472**, 101-107 (2016).

7 Huletsky, A., Loo, V. G., Longtin, Y. *et al.* Comparison of rectal swabs and fecal samples

for the detection of Clostridioides difficile infections with a new in-house PCR assay. *Microbiol. Spectrum*. **12**, e0022524 (2024).

8 Zhang, Y., Walker, R. S. K., Sunna, A., Barber, T. J. & Li, M. Droplet Digital CRISPR for Nucleic Acid Detection. *Adv. Sci.* **13**, e17470 (2026).

9 Gootenberg, J. S., Abudayyeh, O. O., Lee, J. W. *et al.* Nucleic acid detection with CRISPR-Cas13a/C2c2. *Science*. **356**, 438-442 (2017).

10 Gootenberg, J. S., Abudayyeh, O. O., Kellner, M. J. *et al.* Multiplexed and portable nucleic acid detection platform with Cas13, Cas12a, and Csm6. *Science*. **360**, 439-444 (2018).

11 Guan, X., Guo, C., Zhang, J. *et al.* SDS-CRISPR for Single-Nucleotide Variant Detection. *Adv. Sci.* **13**, e75149 (2026).

12 Zhao, J., He, J., Du, H. *et al.* Photo-switchable CRISPR electrochemical system enables de-interferential biosensing signal output. *Biosens. Bioelectron.* **312**, 119067 (2026).

13 Sen, A., Masetty, M., Weerakoon, S. *et al.* Paper-based loop-mediated isothermal amplification and CRISPR integrated platform for on-site nucleic acid testing of pathogens. *Biosens. Bioelectron.* **257**, 116292 (2024).

14 Zhou, T., Huang, R., Huang, M. *et al.* CRISPR/Cas13a Powered Portable Electrochemiluminescence Chip for Ultrasensitive and Specific MiRNA Detection. *Adv. Sci.* **7**, 1903661 (2020).

15 Lee, C. Y., Kim, H., Degani, I. *et al.* Empowering the on-site detection of nucleic acids by integrating CRISPR and digital signal processing. *Nat. Commun.* **15**, 6271 (2024).

16 Ghouneimy, A., Mahas, A., Marsic, T., Aman, R. & Mahfouz, M. CRISPR-Based Diagnostics: Challenges and Potential Solutions toward Point-of-Care Applications. *ACS Synth. Biol.* **12**, 1-16 (2023).

17 Li, Z., Ren, Z., Lin, Y. *et al.* Review of Gastrointestinal Capsule Robots: Materials, Actuation, Diagnostics, and Therapeutics. *Adv. Sci.* **7**, 539-550 (2026).

18 Bhatt, A. S. Digesting New Developments in Biosensors. *N. Engl. J. Med.* **379**, 686-688 (2018).

19 Xu, F., Yan, G., Zhao, K. *et al.* A wireless capsule system with ASIC for monitoring the

physiological signals of the human gastrointestinal tract. *IEEE Trans. Biomed. Circuits. Syst.* **8**, 871-880 (2014).

20 You, S. S., Gierlach, A., Schmidt, P. *et al.* An ingestible device for gastric electrophysiology. *Nat. Electron.* **7**, 497-508 (2024).

21 Mimee, M., Nadeau, P., Hayward, A. *et al.* An ingestible bacterial-electronic system to monitor gastrointestinal health. *Science*. **360**, 915-918 (2018).

22 Inda-Webb, M. E., Jimenez, M., Liu, Q. *et al.* Sub-1.4 cm(3) capsule for detecting labile inflammatory biomarkers in situ. *Nature*. **620**, 386-392 (2023).

23 Zhang, X., Feng, Z., Li, H. *et al.* Ingestible optoelectronic capsules enable bidirectional communication with engineered microbes for controllable therapeutic interventions. *Nat. Microbiol.* **10**, 1841-1853 (2025).

24 De la Paz, E., Maganti, N. H., Trifonov, A. *et al.* A self-powered ingestible wireless biosensing system for real-time in situ monitoring of gastrointestinal tract metabolites. *Nat. Commun.* **13**, 7405 (2022).

25 Min, J., Ahn, H., Lukas, H. *et al.* Continuous Biochemical Profiling of the Gastrointestinal Tract Using an Integrated Smart Capsule. *Nat. Electron.* **8**, 844-855 (2025).

26 Xing, R., Liu, H., Qi, X. & Pan, L. Measuring the process and rate of exogenous DNA degradation during digestion in mice. *Sci. Rep.* **12**, 6463 (2022).

27 Patel, S. K., Pratap, C. B., Jain, A. K., Gulati, A. K. & Nath, G. Diagnosis of Helicobacter pylori: what should be the gold standard? *World J. Gastroenterol.* **20**, 12847-12859 (2014).

28 Ali, A. & AlHussaini, K. I. Helicobacter pylori: A Contemporary Perspective on Pathogenesis, Diagnosis and Treatment Strategies. *Microorganisms*. **12** (2024).

29 Nguyen, P. Q., Soenksen, L. R., Donghia, N. M. *et al.* Wearable materials with embedded synthetic biology sensors for biomolecule detection. *Nat. Biotechnol.* **39**, 1366-1374 (2021).

30 Zou, H., Harrington, J. J., Klatt, K. K. & Ahlquist, D. A. A sensitive method to quantify human long DNA in stool: relevance to colorectal cancer screening. *Cancer Epidemiol., Biomarkers Prev.* **15**, 1115-1119 (2006).

31 Dickinson, B. T., Kisiel, J., Ahlquist, D. A. & Grady, W. M. Molecular markers for

colorectal cancer screening. *Gut*. **64**, 1485-1494 (2015).

32 Jiang, X., Pan, J., Xu, Q. *et al.* Diagnostic accuracy of magnetically guided capsule endoscopy with a detachable string for detecting oesophagogastric varices in adults with cirrhosis: prospective multicentre study. *BMJ*. **384**, e078581 (2024).

33 Arshad, F., Abdillah, A. N., Shivanand, P. & Ahmed, M. U. CeO(2) nanozyme mediated RPA/CRISPR-Cas12a dual-mode biosensor for detection of invA gene in Salmonella. *Biosens. Bioelectron.* **247**, 115940 (2024).

34 Choi, J. H., Lim, J., Shin, M., Paek, S. H. & Choi, J. W. CRISPR-Cas12a-Based Nucleic Acid Amplification-Free DNA Biosensor via Au Nanoparticle-Assisted Metal-Enhanced Fluorescence and Colorimetric Analysis. *Nano Lett.* **21**, 693-699 (2021).

35 Yan, J., Yin, B., Zhang, Q. *et al.* A CRISPR-Cas12a-mediated dual-mode luminescence and colorimetric nucleic acid biosensing platform based on upconversion nanozyme. *Biosens. Bioelectron.* **270**, 116963 (2025).

36 Li, X., Dong, J., Deng, L. *et al.* CRISPR/Cas12a regulated preassembled bulb-shaped G-quadruplex signal unit for FL/CM dual-mode ultrasensitive detection of miRNA-155. *Talanta*. **286**, 127413 (2025).

37 Zha, C. J., Zhang, H. S., Su, M., Nie, Y. G. & Ying, Z. M. Intrinsic crRNA Scaffold Dynamic Reassembly Powered Cas12a Cascade Amplification for Multiplexed Detection. *Anal. Chem.* **98**, 4372-4381 (2026).

38 Zhang, Y., Hao, L., Li, Q. *et al.* Ultrasensitive Wash-Free Homogeneous CRISPR Assay Using Spatial Proximity Chemiluminescence Reporter. *ACS Nano*. **20**, 16001-16015 (2026).

39 van der Veer, H. J., van Aalen, E. A., Michielsen, C. M. S. *et al.* Glow-in-the-Dark Infectious Disease Diagnostics Using CRISPR-Cas9-Based Split Luciferase Complementation. *ACS Cent. Sci.* **9**, 657-667 (2023).

40 Parsonnet, J., Friedman, G. D., Vandersteen, D. P. *et al.* Helicobacter pylori infection and the risk of gastric carcinoma. *N. Engl. J. Med.* **325**, 1127-1131 (1991).

41 Xiao, Y., Zhao, R., Bao, Y. *et al.* Cas12a-assisted split crRNA complex for analysis and detection of diverse entities. *Nucleic Acids Res.* **53** (2025).

42 Larsen, B. B., Kimchi, O., Dunkley, O. R. S. *et al.* RNA structure modulates Cas13

activity and enables mismatch detection. *Nat. Biotechnol.* (2025).

43 Hao, L., Zhao, R. T., Welch, N. L. *et al.* CRISPR-Cas-amplified urinary biomarkers for multiplexed and portable cancer diagnostics. *Nat. Nanotechnol.* **18**, 798-807 (2023).

44 Wu, X., Li, Y., Cao, Y. *et al.* Thermodynamically programmed one-pot CRISPR platform for point-of-care SNP genotyping. *Nat. Commun.* **17** (2026).

45 Even, A., Minderhoud, R., Torfs, T. *et al.* Measurements of redox balance along the gut using a miniaturized ingestible sensor. *Nat. Electron.* **8**, 856-870 (2025).

46 Asci, C., Del-Rio-Ruiz, R., Sharma, A. & Sonkusale, S. Ingestible pH Sensing Capsule with Thread-Based Electrochemical Sensors. *Proc. IEEE Sens.* **2022** (2022).

47 Hou, B., Yi, L., Hu, D. *et al.* A swallowable X-ray dosimeter for the real-time monitoring of radiotherapy. *Nat. Biomed. Eng.* **7**, 1242-1251 (2023).

48 Sharma, S., Cai, Y., Moon, I. *et al.* A miniaturized ingestible temperature sensor for continuous internal monitoring. *Nat. Electron.* **9**, 956-968 (2026).

49 Singh, N., Lane, S., Yu, T. *et al.* A generalized platform for artificial intelligence-powered autonomous enzyme engineering. *Nat. Commun.* **16**, 5648 (2025).

50 Cheng, Y., Duong, H. T. T., Hu, Q., Shameem, M. & Tang, X. C. Practical advice in the development of a lyophilized protein drug product. *Antibody Ther.* **8**, 13-25 (2025).

Supplementary Files

This is a list of supplementary files associated with this preprint. Click to download.

- VideoS1.Invitrosamplingbytheelectroniccapsule.mp4
- VideoS5.Tetheredretrievaloftheelectroniccapsuleinapig.mp4
- VideoS4.Endoscopicvisualizationofgastricsamplingbytheelectroniccapsuleinapig.mp4
- VideoS3.Endoscopicvisualizationofgastricsamplingbytheelectroniccapsuleinadog.mp4
- VideoS2.Invitroopticalresponseoftheelectroniccapsule.mp4
- SupplementaryInformation.pdf